

Radio-Frequency Plasma-Assisted Pulsed Laser Deposition of TiO_xN_y on Multi-walled Carbon Nanotubes: A Structural and Compositional Study

E. Pajootan¹, S.A. Alolabi², S. Coulombe¹ and S. Omanovic¹

¹Department of Chemical Engineering, McGill University, Montreal, Quebec, Canada

²Department of Applied Physics, Eindhoven University of Technology, The Netherlands

Abstract:

Titanium oxynitride thin coatings on multi-walled carbon nanotubes were synthesized by a radio-frequency plasma-assisted pulsed laser deposition method using a titanium target in an Ar/N₂ environment at 30 mTorr. X-ray photoelectron spectroscopy (XPS) measurements indicated an increase of oxygen containing species in the film by adding RF plasma. Scanning electron microscopy (SEM) images showed morphological alteration from layer-by-layer to stepped coating structure.

Keywords: RF plasma, pulsed laser deposition, thin coating, titanium oxynitride.

1. Introduction

Titanium based coatings and nanoparticles, such as titanium nitride (TiN) and titanium oxynitride (TiO_xN_y), offer highly desirable properties such as hardness, excellent wear resistance, high melting point, thermodynamic stability, high conductivity, oxidation resistance and corrosion resistance. Consequently, these thin films are being widely used as coating materials, cutting and drilling tools, diffusion barrier in integrated circuits, contact material in semiconductors, and catalyst substrates in electrochemical applications [1, 2].

The relatively high conductivity, corrosion and oxidation resistance of TiN films make them an attractive option in energy storage applications. Moreover, TiN is resistant to oxidation, due to the native oxide/oxynitride on its surface. This layer of native oxide/oxynitride is formed due to a thermodynamically favourable oxidation that occurs when TiN is exposed to air and prevents further oxidation of the surface [3, 4]. TiN coatings are mainly produced by magnetron sputtering or chemical vapour deposition (CVD) with a reaction between TiCl_4 and NH_3 . The latter however, faces problems such as chlorine impurity incorporation and high temperature requirements (greater than 600 °C). More advanced methods such as plasma-enhanced CVD and physical vapour deposition (PVD) provide suitable alternatives that circumvent these problems [5]. A less studied physical vapour deposition method for the synthesis of TiN films is pulsed laser deposition (PLD). In PLD, the short pulse duration and high fluence laser beam focused on a titanium target produces an expanding metal vapor plasma plume containing ground- and excited-state neutral atoms, ions and electrons. With a substrate facing the target, dense films can be deposited under vacuum conditions, whereas nanoparticles with controlled size can be deposited in an inert gas environment at higher pressures [6].

In this study, the combination of PLD with a capacitively-coupled radio-frequency (CCRF) plasma called radio-frequency plasma-assisted pulsed laser deposition (RF-PAPLD) was investigated in the synthesis of TiO_xN_y . The incorporation of plasma influences the morphology, roughness and composition of the deposited

layers [7]. To the authors' knowledge, synthesis of titanium nitride and oxynitride has not been yet investigated by this method. X-ray photoelectron spectroscopy (XPS) and scanning electron microscopy (SEM) imaging was used as the main characterization techniques to investigate the composition and morphology of the deposited layer. This work is part of a research project on the production of Pt-based catalysts deposited on MWCNTs for direct methanol fuel cells. The altered properties of a TiN thin film deposited by RF-PAPLD could improve the stability and durability of the electrocatalyst for methanol oxidation reaction. Therefore, TiO_xN_y are deposited on the surface of MWCNTs as a sublayer for further deposition of platinum nanostructures which act as the electrocatalyst.

2. Experimental

Thin films of TiO_xN_y were synthesized by RF plasma-assisted pulsed laser deposition. A schematic representation of the experimental setup is shown in Fig. 1. A Quantel Brilliant B10 (Nd:YAG, wavelength: 355 nm, frequency: 10 Hz, pulse duration: 4-6 ns) laser beam is focused on a titanium target. The target consisted of a Ti coupon mounted on a 9 cm O.D. stainless steel disc. The substrate consisted of CVD-grown MWCNT-covered stainless steel mesh coupons mounted on a 6 cm O.D. stainless steel disc [8]. The target-to-substrate distance was set to 3 cm in all experiments.

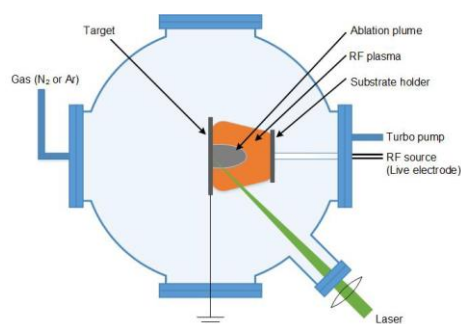


Fig. 1. Schematic representation of the RF-PAPLD setup.

A continuous wave volumetric capacitively-coupled radio-frequency (CCRF) plasma was produced using the target as the RF-powered (13.56 MHz) electrode and the substrate as ground. The chamber was flushed with argon and pumped down to a base pressure of 10^{-5} Torr, prior to thin film deposition, and repressurized to 30 mTorr for the deposition. The RF power level was set at 10 W for all experiments. Three combinations of experiments were performed: i) PLD in N_2 , ii) PLD in Ar, and iii) RF-PAPLD in N_2 .

3. Results and discussions

SEM imaging was used to investigate the morphology of titanium nanostructures deposited on the surface of carbon nanotubes. SEM images (Fig. 2) of titanium ablated in N_2 and/or Ar atmosphere show that MWCNTs are uniformly coated with titanium nanostructures. The morphology of these coatings suggests the layer-by-layer or multilayer growth mode of thin film on the substrate. The interesting stepped coating structure is observed when the sample was prepared by RF-PAPLD in N_2 . It can be seen that the interaction of RF plasma and the laser induced plasma plume changed the growth mode of the thin film from layer-by-layer to step-flow [9]. It is reported that the layers growth in the step-flow mode have relatively high crystal perfection due to the prevention of defects resulted from coalescence [10]. This requires further study of the crystalline structure of the synthesized film.

The chemical composition and uniformity of the thin film synthesized by RF-PAPLD in N_2 were characterized at multiple depths using the XPS through successive argon etching steps, for a total time of 13 min. Ti2p, O1s and N1s were identified from the survey scans. Fig. 3 displays the atomic percentages of Ti2p, N1s and O1s as a function of the argon etching time. As can be seen, the composition of the sample is uniform over its depth after approximately 360 s of argon etching, with relatively constant atomic percentages of Ti, O and N. The surface of the thin film is mainly composed of TiO_2 . This is the expected native oxide layer that forms on the surface from the atmospheric oxidation of TiN:



This reaction is thermodynamically favourable (Gibbs free energy ΔG° at 20 °C is $-611.8 \text{ kJ mol}^{-1}$) [4].

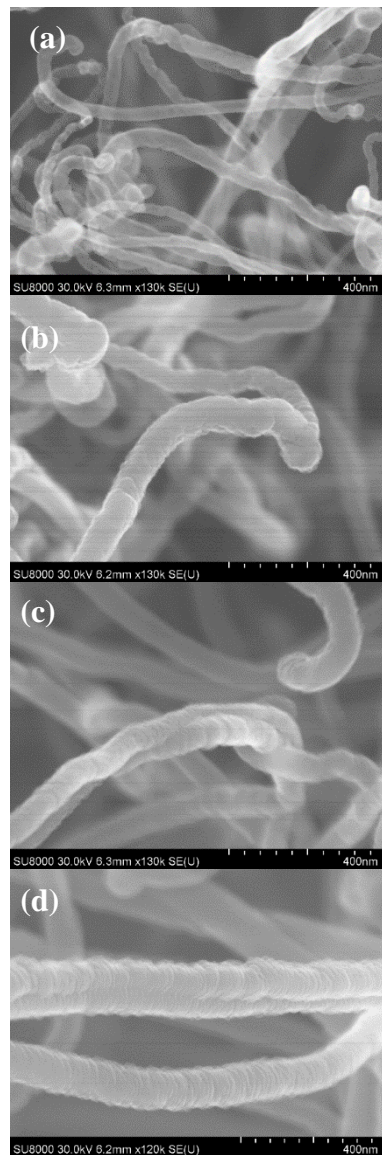


Fig. 2. SEM images of (a) MWCNTs, (b) PLD of Ti in Ar, c) PLD of Ti in N_2 , and d) RF-PAPLD of Ti in N_2 .

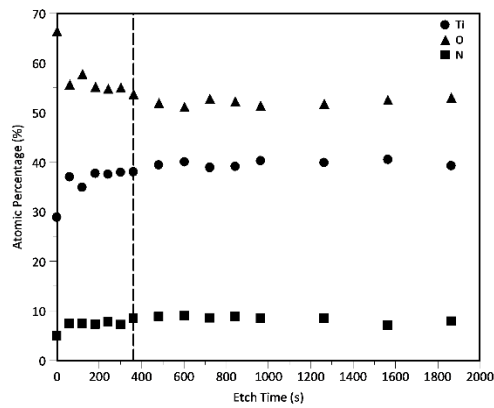


Fig. 3. Percentage of Ti, O and N atoms versus argon etching duration obtained with RF-PAPLD in N_2 .

Deconvoluted Ti2p XPS spectra obtained for all samples (PLD in N_2 , PLD in Ar, and RF-PAPLD in N_2) after argon etching for 360 s are shown in Fig. 4. The calculated TiN, TiO_2 , TiON and TiO percentages are reported in Table 1. The thin film deposited by PLD in Ar is nitrogen-free. The Ti2p scan shows two different titanium oxide states of TiO and TiO_2 . The oxide state of TiO was only detected in the thin film deposited with the Ar background gas.

The compositional analysis for the sample deposited by PLD in N_2 revealed that this thin film is composed of 83% of TiN due to the interaction of nitrogen gas and laser-induced plasma plume, while the existence of TiON and TiO_2 is also evident due to the formation of the native oxide film. The deconvolution of Ti2p spectra for the sample synthesized by RF-PAPLD in N_2 shows an increase in the percentage of oxygen containing species (TiO_2 and TiON).

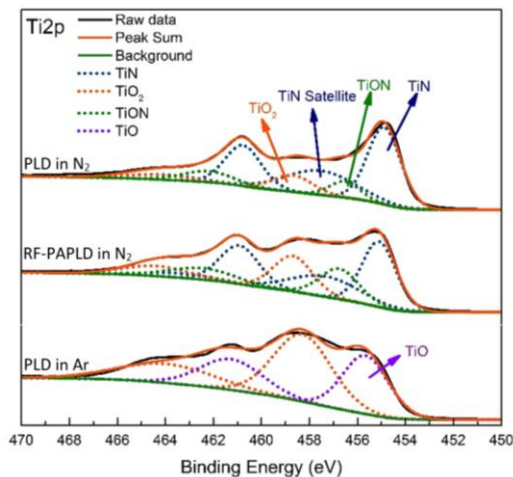


Fig. 4. Deconvoluted Ti2p XPS spectra of samples prepared by PLD in N_2 , PLD in Ar, and RF-PAPLD in N_2 .

Table 1. Percentage of TiN, TiO_2 , TiON and TiO peaks from the deconvoluted Ti2p scans.

Sample	TiN (%)	TiO_2 (%)	TiON (%)	TiO (%)
Ti ablated in argon- no plasma	—	53.7	—	46.3
Ti ablated in nitrogen-plasma at 10W	69.8	15.1	15.1	—
Ti ablated in nitrogen-no plasma	83.0	7.5	9.5	—

Optical emission spectroscopy (OES) was used to qualitatively assess the presence of oxygen in the chamber. Fig. 5 shows an emission spectrum collected during a RF-PAPLD experiment using N_2 as the background gas. The first and second positive emission bands of N_2 can be identified. The low intensity peaks present in the vicinity of 500 and 525 nm are related to titanium emission lines [11]. The emission line at 309 nm corresponds to the hydroxyl radical (OH), which indicates the presence of water in the chamber. Similar observation and effect have been previously reported by other researchers [12, 13]. Therefore, the presence of hydroxyl radicals in the chamber results in the formation of more oxygen containing species (TiO_2 and TiON) in the deposited film.

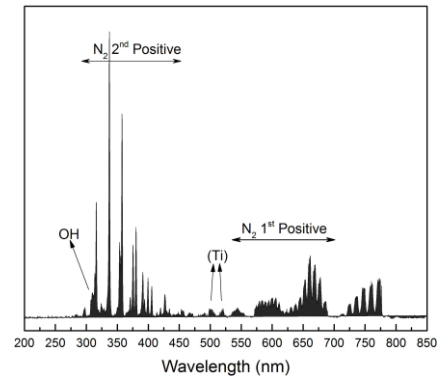


Fig. 5. Optical emission spectrum obtained in a RF-PAPLD experiment with N_2 as background gas.

4. Conclusion

PLD and RF-PAPLD were employed to synthesize thin films of titanium nanostructures with different morphologies, and oxygen and nitrogen contents. Uniform coatings with similar composition through the depth of the film were synthesized. The RF-PAPLD technique allows alteration of the film morphology as well as its composition. This method can be used to tune the properties of the synthesized coatings in accordance with the desired application.

5. References

- [1] Saha, N.C. and H.G. Tompkins, Journal of Applied Physics, **72**, 7 (1992).

- [2] Avasarala, B. and P. Haldar, *International Journal of Hydrogen Energy*, **36**, 6 (2011).
- [3] Avasarala, B. and P. Haldar, *Electrochimica Acta*, **55**, 28 (2010).
- [4] Milošv, I., et al., *Surface and Interface Analysis*, **23**, 7-8 (1995).
- [5] Jeon, H., et al., *Journal of Vacuum Science & Technology A*, **18**, 4 (2000).
- [6] Trelenberg, T.W., et al., *Applied Surface Science*, **229**, 1 (2004).
- [7] De Giacomo, A., et al., *Applied Surface Science*, **186**, 1 (2002).
- [8] Hordy, N., et al., *Carbon*, **63**, (2013).
- [9] Rijnders, G.a.B., D. H., John Wiley & Sons, Inc., (2006).
- [10] Byrappa K., O.T., Springer-Verlag Berlin Heidelberg, (2003),
- [11] W.M. Haynes, e.C.H.o.C.a.P.C.P., 97th edition, 2016.,
- [12] Ohkawa, K., A. Ueno, and T. Mitsuyu, *Journal of Crystal Growth*, **117**, 1 (1992).
- [13] Hong, Y.J., et al., *Journal of Instrumentation*, **7**, 03 (2012).